Nonlinear Dyn (2016) 84:959–975
DOI 10.1007/s11071-015-2542-y

ORIGINAL PAPER

An approach combining periodicity ratio and secondary Poincaré map for characteristics diagnosis of nonlinear oscillatory systems

Tousheng Huang · Liming Dai · Huayong Zhang

Received: 20 January 2015 / Accepted: 1 December 2015 / Published online: 31 December 2015

Abstract A secondary Poincaré map approach is developed in this research for diagnosing the nonlinear characteristics such as quasiperiodic and chaotic responses of a dynamic system. With the secondary Poincaré map approach developed, an approach combining the periodicity ratio method and the secondary Poincaré map approach is established such that all the dynamical characteristics of a nonlinear dynamic system can be systemically and completely identified. An example of an ecological oscillatory system is presented in the research to demonstrate the application of the combined approach. Periodic–quasiperiodic–chaotic region diagrams are generated with the employment of the approach, for a global characterization of this system with consideration of large ranges of system parameters. The approach developed in this research demonstrates effectiveness and efficiency in completely diagnosing the complex dynamical characteristics of nonlinear oscillatory systems, such as periodic, quasiperiodic, chaotic responses of the systems together with those in between periodic and chaotic responses.

T. Huang · H. Zhang
Research Center for Engineering Ecology and Nonlinear Science, North China Electric Power University, Beijing 102206, People's Republic of China

T. Huang · L. Dai (✉)
Industrial Systems Engineering, University of Regina, Regina, SK S4S 0A2, Canada
e-mail:liming.dai@uregina.ca

Keywords Nonlinear oscillatory system · Nonlinear characteristics diagnosis · Ecological systems · Periodicity · Quasiperiodicity · Chaos · PR method · Poincaré map

1 Introduction

Nonlinear oscillatory systems widely exist in reality. In scientific and engineering areas, many important nonlinear oscillatory systems are found, such as spring vibration system, pendulum system [1], Duffing system [2,3], circuit system [4,5], and ecological predator–prey system [6,7]. The research works on nonlinear oscillatory systems demonstrate that these systems may exhibit abundant nonlinear characteristics, including multiplicity of attractors, quasiperiodic behavior, and deterministic chaos [4–10]. Moreover, many complex behaviors can emerge in the nonlinear oscillatory systems, for example, occurrence of multi-scroll attractors in some chaotic oscillators [4,5].

For diagnosing periodic and non-periodic dynamical characteristics of the nonlinear oscillatory systems, a few available methods, empirical or theoretical, can be employed [11–13]. As described in literature, the most often used methods for characteristics diagnosis are Lyapunov exponent, fractal dimension, and Poincaré map [12,14].

Lyapunov exponent of a dynamical system describes a quantity which characterizes the average exponential rate of divergence or convergence of nearby trajec-

tories in phase space [15]. The employment of Lyapunov exponent provides efficient determination for many types of dynamical behaviors [16,17]. It should be noticed that the employment of Lyapunov exponents to dynamical systems needs that the trajectories of the system are globally bounded. But generally, the global boundedness of a nonlinear system is hard to prove analytically. Therefore, the two necessary conditions for identifying chaos of nonlinear systems, global boundedness and at least one Lyapunov exponents being positive, are both based on numerical simulation [18].

Fractal dimension is an effective method for describing fine structures of strange attractors [14]. For the cases of equilibrium, period, and quasiperiod, the dimension is integer, whereas for the chaotic case, fractional dimension emerges. There are mainly four ways to generalize dimension to the fractional case, capacity dimension, information dimension, correlation dimension, and Lyapunov dimension [12,14,19,20].

Poincaré map is also widely applied to study the characteristics of nonlinear dynamical systems using graphical representation [21,22]. This map is produced by considering successive intersections of a trajectory of the nonlinear dynamical system with a codimension-one surface, a Poincaré section, of the phase space [23]. According to the graphical feature of the visible points in Poincaré maps, the periodic, quasiperiodic, and chaotic oscillations can be distinguished.

For quantitatively describing the periodicity of the dynamical behaviors of nonlinear systems, a periodicity ratio (PR) method was developed [13,24]. The determination of the periodicity ratio is based on examining the overlapping points with respect to the total number of points in a Poincaré map. The overlapping points in a Poincaré map describe that one system considered repeatedly returns to its original state, i.e., periodicity. The higher the periodicity ratio value is, the more periodic is the dynamical behavior. For a perfect periodic system, the periodicity ratio must be one, whereas for a quasiperiodic or chaotic behavior, the periodicity ratio approaches zero.

The behavior of non-chaotic, non-periodic, and non-quasiperiodic has been recognized by the researchers in the areas of nonlinear science. The intermittent behavior of nonlinear dynamical systems is a typical behavior falling in this category [25,26]. Almost periodic phenomena, the dynamic behavior in between periodic and quasiperiodic behaviors is also seen in the literature [27–29]. The PR method has power in defining the dynamical behaviors between 0 and 1, which are the cases that are neither periodic nor chaotic or quasiperiodic behaviors. Such cases of dynamical behaviors are hard to be described by other methods available for diagnosing nonlinear systems. However, with the employment of the PR method, quasiperiodicity and chaos cannot be distinguished, since the periodicity ratios of these two cases are both zero.

With the considerations described above and taking the advantages of the PR method, a new mapping approach named the secondary Poincaré map will be established in this research, in order to improve the capability of diagnosing the dynamical characteristics of nonlinear systems. Like the PR method, the establishment of the new map is also based on the feature of points distributed in the Poincaré map for different dynamical behaviors. The new secondary Poincaré map approach reduces the non-chaotic oscillations into finite points shown in the map and simultaneously keeps the main properties of chaos in the map: a cloud of unorganized, randomly points or Cantor-set-like patterns. In the literature, very few researchers performed works in establishing second-order Poincaré maps [12,30,31]. However, their works mainly considered how to reduce the quasiperiodic solutions of nonlinear oscillatory systems to a point in a map, and scarcely referred how to diagnose the chaotic oscillation with their approach.

With the employment of the secondary Poincaré map, to be developed combining with the PR method, the nonlinear characteristics of periodically forced oscillatory systems will be diagnosed. The development of the combined PR method and secondary Poincaré map approach will be described in Sect. 2. An example of an ecological system will be used in Sect. 3 to demonstrate the application of the approach in diagnosing the nonlinear oscillatory characteristics of the nonlinear system. Discussion and conclusion will be given in Sect. 4.

2 Methods of investigation: PR method and secondary Poincaré map approach

Consider a two-dimensional periodically forced oscillatory system

$$\frac{\mathrm{d}\vec{\boldsymbol{x}}}{\mathrm{d}t} = \vec{\boldsymbol{g}}\left(\vec{\boldsymbol{x}}, t\right), \tag{1}$$

in which variable $\vec{\boldsymbol{x}}$ and function $\vec{\boldsymbol{g}}$ represent vectors with two components, $\vec{\boldsymbol{x}} = (x_1, x_2)$ and $\vec{\boldsymbol{g}} = (g_1, g_2)$. Supposing the periodically forced oscillatory system has a periodic excitation of period T. Let $\vec{\boldsymbol{x}}(t)$ be the solution of this system which starts from an initial condition $\vec{\boldsymbol{x}}_0 = (x_{10}, x_{20})$.

2.1 PR method

The PR method is developed by Dai [13] and Dai and Singh [24], for diagnosing the nonlinear behavior and quantitatively measuring the periodicity of a dynamic system. For periodically forced systems, the periodically forced terms play an important role in determining system behaviors. Rinaldi et al. recorded introducing periodically forced parameters can change attractor properties of the original system, for example, equilibrium point transforming to limit cycle, limit cycle transforming to quasiperiodic behavior [8]. According to previous studies of Ueda and Khammari et al. [32,33], Poincaré sections of system (1) can be obtained by sampling points from $\vec{\boldsymbol{x}}(t)$ at regular time interval, and the regular time interval can be set as period T. Such method of constructing Poincaré sections for periodically forced systems is widely applied in literature [13,32–34]. Based on the above description, a time-sampled sequence of points in the Poincaré section is described by

$$X_0 = \{\vec{\boldsymbol{x}}(t_1), \vec{\boldsymbol{x}}(t_2), \ldots, \vec{\boldsymbol{x}}(t_k)\}, \tag{2}$$

in which

$$t_k = t_1 + (k-1)T.$$

t_1 is the time at which the first point is sampled on $\vec{\boldsymbol{x}}(t)$, and $k \in Z$, Z is the set of integers. For convenience, a mapping f_0 is used to denote the transformation from $\vec{\boldsymbol{x}}(t)$ to X_0,

$$X_0 = f_0(\vec{\boldsymbol{x}}(t)). \tag{3}$$

According to the PR method developed in Dai [13] and Dai and Singh [24], the points appearing in the corresponding Poincaré map are classified into two sorts: overlapping points and non-overlapping points. The overlapping points state that a visible individual point in the Poincaré map is actually overlapping with a group of periodic points spanned apart by a period along the time axis [34]. The other points in the Poincaré map except the overlapping points are non-overlapping points. The periodically overlapping points in the Poincaré map describe that corresponding dynamical system considered repeatedly returns to its original state, i.e., periodicity. The ratio of the periodically appearing overlapping points with respect to the total number of points in the Poincaré map is defined as periodicity ratio (PR).

In X_0, two points $\vec{\boldsymbol{x}}(t_m)$ and $\vec{\boldsymbol{x}}(t_n)$ are called overlapping points, if they satisfy

$$\vec{\boldsymbol{x}}(t_m) = \vec{\boldsymbol{x}}(t_n) \, (1 \le m, n \le k, m, n \in Z), \tag{4}$$

i.e.,

$$x_1(t_m) = x_1(t_n),$$
$$x_2(t_m) = x_2(t_n) \, (1 \le m, n \le k, m, n \in Z).$$

Moreover, the number of all the overlapping points (NOP) of X_0 can be calculated by

$$\mathrm{NOP} = \xi(1) + \sum_{m=2}^{k} \xi(m) \cdot Q_1\left(\prod_{n=1}^{m-1}\left\{X_{mn}^1 + X_{mn}^2\right\}\right) \quad (1 \le m, n \le k, m, n \in Z), \tag{5}$$

in which

$$X_{mn}^1 = |x_1(t_m) - x_1(t_n)|, \tag{6a}$$
$$X_{mn}^2 = |x_2(t_m) - x_2(t_n)|, \tag{6b}$$
$$Q_1(y) = \begin{cases} 0, & \text{if } y = 0 \\ 1, & \text{if } y \neq 0 \end{cases}, \tag{6c}$$
$$Q_2(y) = \begin{cases} 1, & \text{if } y = 0 \\ 0, & \text{if } y \neq 0 \end{cases}, \tag{6d}$$
$$\xi(m) = \left\{\sum_{n=m}^{k} Q_2\left(X_{mn}^1\right) \cdot Q_2\left(X_{mn}^2\right)\right\} \cdot Q_1 \times \left(\sum_{n=m}^{k}\left[Q_2\left(X_{mn}^1\right) \cdot Q_2\left(X_{mn}^2\right)\right] - 1\right). \tag{6e}$$

With the calculated NOP, the periodicity ratio of the nonlinear oscillatory system considered in this research is defined as

$$\mathrm{PR} = \lim_{k \to \infty} \frac{\mathrm{NOP}}{k}. \tag{7}$$

The periodicity ratio thus defined describes the degree of periodicity for a dynamical system. For a perfect periodic oscillation, all the points in the Poincaré

map are overlapping points; therefore, the periodicity ratio must be 1, whereas for a quasiperiodic or chaotic oscillation, the periodicity ratio approaches zero. When both overlapping and non-overlapping points exist in the Poincaré map, the periodicity ratio (PR) may lie between 0 and 1. For such cases, the dynamical behaviors hold the properties of periodic and non-periodic oscillations simultaneously. Therefore, such behaviors are not periodic, quasiperiodic, or chaotic. The PR values quantify the periodicity of a nonlinear system; when PR is close to 1, the corresponding dynamical behavior is close to perfectly periodic.

2.2 Secondary Poincaré map

Noticing that the PR values for quasiperiodic and chaotic oscillations are both zero. It means PR method is incapable of distinguishing quasiperiodic and chaotic oscillations for nonlinear oscillatory systems. To cover this shortage, a secondary Poincaré map is developed as shown in the following.

According to graphical feature shown in a Poincaré map, the dynamic behavior of a system can be recognized. It is well known that a finite number of visible points describe periodic oscillations, and a continuous closed orbit describes the quasiperiodic oscillations [35]. If, on the other hand, a dynamical behavior is chaotic, the Poincaré map appears as a cloud of unorganized, randomly points or Cantor-set-like patterns in the phase plane [35].

Such recognition of dynamical behaviors is based on the structure of visible points shown in Poincaré map. The visible points for a Poincaré map of system (1) can be defined as follows.

Definition 1 If $\vec{\boldsymbol{x}}\left(t_{m_1}\right), \vec{\boldsymbol{x}}\left(t_{m_2}\right), \ldots, \vec{\boldsymbol{x}}\left(t_{m_n}\right)$ $(2 \leq n \leq k, n \in Z)$ are overlapping points in the Poincaré map, removing the overlapping points $\vec{\boldsymbol{x}}\left(t_{m_2}\right), \ldots, \vec{\boldsymbol{x}}\left(t_{m_n}\right)$ from X_0. A new set of points,

$$X_1 = \left\{\vec{\boldsymbol{x}}\left(t_{u_1}\right), \vec{\boldsymbol{x}}\left(t_{u_2}\right), \ldots, \vec{\boldsymbol{x}}\left(t_{u_s}\right)\right\} \quad \left(u_i \in Z, 1 \leq i \leq s\right), \tag{8}$$

is used to represent the visible points in the Poincaré map and s is the number of the visible points. Moreover, a map f_1 is defined to describe the transformation from X_0 to X_1,

$$f_1\left(X_0\right) = X_1. \tag{9}$$

The secondary Poincaré map approach proposed is based on the introduction of parallel straight lines in a Poincaré map. If a straight line introduced intersects with X_1 in the Poincaré map, for the case of periodic and quasiperiodic oscillations, it will lead to finite number of intersecting points, whereas for the case of chaos, it may have infinite number of intersecting points theoretically. The map such constructed is based on the conventional Poincaré map method and therefore named as the secondary Poincaré map in the present research. The purpose of the secondary Poincaré map approach is to transform the periodic and quasiperiodic oscillations into finite points and to transform the chaos of the system into infinite number of points in the map.

Definition 2 Consider a straight line,

$$Y_0 : ax_2 = bx_1 + c, \tag{10}$$

then $X_1 \cap Y_0$ describes the intersecting points of Y_0 and X_1 in the Poincaré map of system (1). The number of the intersecting points of X_1 and Y_0 is defined by

$$N_0 = C\left(X_1 \cap Y_0\right), \tag{11}$$

in which C is a function, representing the cardinal number of a set.

As described in literature, the visible points of chaos in the Poincaré map distribute as cloud or Cantor dust. Therefore for the chaotic oscillations, when k approaches infinite, for any fixed parameters of a and b, there must exist such value of parameter c, making that

$$\lim_{k\to\infty} \underset{\text{for } \forall a,b,\exists c}{N_0} = \aleph_0, \tag{12}$$

in which $\aleph_0$ is the cardinal number of the set of natural numbers.

Definition 3 Consider a group of straight lines which have the same slope,

$$Y = \left\{Y_i \left| a\left(x_2 - x_2\left(t_{u_i}\right)\right) = b\left(x_1 - x_1\left(t_{u_i}\right)\right), \right. \right. \\ \left. 1 \leq i \leq s, i \in Z\right\}, \tag{13}$$

define

$$N_i = C\left(X_1 \cap Y_i\right), \tag{14}$$

and

$$N = \max_{1\leq i\leq s} \lim_{k\to\infty} N_i. \tag{15}$$

According to the previous description, for periodic and quasiperiodic oscillations, N is a finite number, but for chaotic oscillations, N is infinite theoretically.

Definition 4 According to different cases of N, a mapping f_2 is defined by

$$X_2 = f_2|_Y(X_1) = \begin{cases} \bigcup_i (X_1 \cap Y_i) \text{ for all } i, \lim_{k\to\infty} N_i = N, 1 \le i \le s, i \in Z, \text{ if } N = \aleph_0 \\ X_1 \cap Y_i \text{ for any } i, \lim_{k\to\infty} N_i = N, 1 \le i \le s, i \in Z, \text{ if } N < \aleph_0 \end{cases} \quad (16)$$

This mapping obtains an intersection surface of X_1 and Y. For the case of chaos, X_2 is an infinite set based on the definition specified, whereas for the periodic case, a few points appear in X_2. However, in some situations of quasiperiodic oscillations, there may exist some subset of X_1 forming a curve in the Poincaré map which has overlapping part with Y_i for some i, $1 \le i \le s, i \in Z$. This may lead to a fault result when distinguishing the quasiperiodic oscillation from the chaotic oscillation. To avoid such situation, an amendment can be performed on the basis of X_2.

Definition 5 For

$$X_2 = \left\{\vec{x}\left(t_{l_1}\right), \vec{x}\left(t_{l_2}\right), \ldots, \vec{x}\left(t_{l_r}\right)\right\} (r \in Z), \quad (17)$$

consider a group of straight lines which are perpendicular to Y,

$$\tilde{Y} = \left\{\tilde{Y}_i \,|b\left(x_2 - x_2\left(t_{l_i}\right)\right) = -a\left(x_1 - x_1\left(t_{l_i}\right)\right), \; 1 \le i \le r, i \in Z\right\}. \quad (18)$$

Let

$$\tilde{N}_i = C\left(X_2 \cap \tilde{Y}_i\right), \quad (19)$$

and

$$\tilde{N} = \max_{1\le i\le s} \lim_{k\to\infty} \tilde{N}_i, \quad (20)$$

then an amended set X_3 on the basis of X_2 is defined by

$$X_3 = f_2|_{\tilde{Y}}(X_2). \quad (21)$$

Summarizing the above descriptions, the secondary Poincaré map f can now be described as the following.

Definition 6 f is defined by

$$f = f_2|_{\tilde{Y}} \circ f_2|_Y \circ f_1 \circ f_0, \quad (22)$$

and

$$X_3 = f\left(\vec{x}(t)\right). \quad (23)$$

According to above description, as k approaches infinite, for chaotic oscillations, X_3 is a union set of a few infinite sets. Therefore, infinite number of points exist in X_3 for chaotic oscillations. On the contrary, for non-chaotic oscillations, there are only finite number of points in X_3.

3 Application of the secondary Poincaré map approach

The main goal for the proposed combined method is to diagnose the nonlinear characteristics of periodically forced oscillatory systems. In ecology field, periodically forced oscillatory systems widely exist, due to the influences of periodic seasonal variations. For example, variation of precipitation greatly affects vegetation dynamics in arid and semiarid dryland during a year [8]; seasonal cycle of temperature and light and fish predation imposes strong influence on the predator–prey interaction between algae and zooplankton [36]; and so on. Accordingly, diagnosing the nonlinear characteristics of periodically forced ecological systems has significance for better comprehending the population dynamics in nature.

Phytoplankton–zooplankton oscillations are one of the most common and important phenomena in nature. Great efforts have been made on this subject of ecology and many models have been established to investigate the phytoplankton–zooplankton interactions [36,37]. Some researchers argued that a few models sought to contain as many as physical and biological mechanisms, however, frustrated accurate agreement with observations due to the uncertainties in the values of too many parameters [38]. Contrarily, some simple models describing the generic mechanisms were valid in explaining natural behaviors, such as plankton blooms. Among the simple models, Truscott–Brindley model made notable progress in modeling plankton population dynamics [39]. In this research, the seasonally forced T–B model is investigated with the application of the combined approach of PR method and secondary Poincaré map [38]. The original T–B model can be described as

$$\frac{\mathrm{d}P(t)}{\mathrm{d}t} = rP\left(1-\frac{P}{K}\right) - R_m\frac{P^2}{\alpha^2+P^2}Z, \tag{24a}$$

$$\frac{\mathrm{d}Z(t)}{\mathrm{d}t} = \gamma R_m\frac{P^2}{\alpha^2+P^2}Z - uZ, \tag{24b}$$

in which P and Z are the concentrations of phytoplankton and zooplankton populations, respectively; r and K are the growth rate and carrying capacity of the phytoplankton population; R_m is the maximum predation rate; α is the half-saturation concentration; γ is the conversion efficiency; u is the death rate of the zooplankton.

To describe the seasonal forcing in the T–B model, Gao et al. [38] took an assumption that the parameters of above model should be described as periodic functions of time. According to Gao et al. [38], two parameters, r and u, are transformed into periodically time-varying functions, $r(t)$ and $u(t)$, which can be described by the following,

$$r(t) = r_0(1 + A\sin(w_1 t)), \tag{24c}$$

$$u(t) = u_0(1 + B\sin(w_2 t)), \tag{24d}$$

in which r_0 and u_0 are average values of $r(t)$ and $u(t)$, A and B determine the magnitude of the seasonality, w_1 and w_2 are the angular frequencies of seasonal variations. According to Rinaldi et al. [8], periodic variation of $r(t)$ is mainly relative to the periodic variation of nutrients available to the phytoplankton community, whereas periodic presence of a superpredator (such as fish) exploiting the zooplankton community gives rise to periodic variations of $u(t)$. Since $r(t)$ and $u(t)$ are influenced by the factors of seasonal variations which may rely on different time scales, w_1 and w_2 may take different values.

To demonstrate the application of the approach combining periodicity ratio and secondary Poincaré map methods in diagnosing the nonlinear characteristics of dynamical systems, the above ecological oscillatory system of phytoplankton and zooplankton is investigated. Numerical simulations are performed based on the methods described in Sect. 2. In the simulations, the parameter values of Gao et al. [38] and Truscott and Brindley [39] are used, i.e., $r_0 = 0.3, K = 108, R_m = 0.7, \alpha = 5.7, \gamma = 0.05, A = 0.2$, and $B = 0.2$. u_0, w_1 and w_2 are kept varying when performing numerical simulations. In performing all the numerical calculations, the fourth-order Runge–Kutta method is employed.

3.1 Utilization of PR method

In performing the secondary Poincaré map approach, the PR method needs to be utilized firstly. For the utilization of PR method in numerical simulations, three important conditions should be noticed.

(1) Running time of numerical programs for solving Eq. (24), t. t is directly related to the total number of points in the Poincaré map.
(2) The time for starting sampling points from $\vec{\boldsymbol{x}}(t)$, t_1. Transient dynamics may greatly influence the calculation of PR values. To remove the effects of transient dynamics, t_1 is set to ensure the solution be close enough to the attractor. In addition, the total number of points in a Poincaré map is therefore the integer value of $(t - t_1)/T$.
(3) Due to the restriction of numerical computation, the overlapping points defined in Sect. 2.1 are difficult to be numerically captured. Therefore, a tolerance, ε, is set for numerically determining overlapping points in the Poincaré map. ε is dependent on t, t_1 and the error of Runge–Kutta method. On the other hand, the value of ε directly affects the computational accuracy of PR values. Applying the tolerance, Eq. (4) is changed into the following,

$$\left|\vec{\boldsymbol{x}}(t_m) - \vec{\boldsymbol{x}}(t_n)\right| < \boldsymbol{\varepsilon}\ (1 \le m, n \le k, m, n \in Z). \tag{25}$$

In determining for the specific values of t, t_1 and ε, the research results of Gao et al. [38] are employed in the present research. The authors studied the same ecological system considered in the present research and reported periodic, quasiperiodic, and chaotic oscillations with given system parameters. The values of t, t_1 and ε are therefore determined by comparing the results of Gao et al. [38] and that of the PR approach. The values are determined when the results of the two independent approaches are satisfactorily agreed, though more accurate results can be reached if smaller tolerance is selected. The final values such determined for the parameters used in the research are $t = 2.5 \times 10^5, t_1 = 1 \times 10^3$, and $\varepsilon = 1 \times 10^{-4}$.

With the conditions provided above, the PR method can now be applied to quantitatively diagnose the nonlinear characteristics of the oscillatory ecological system considered. Figures 1, 2, 3, and 4 illustrate four types of main dynamical oscillations of the system.

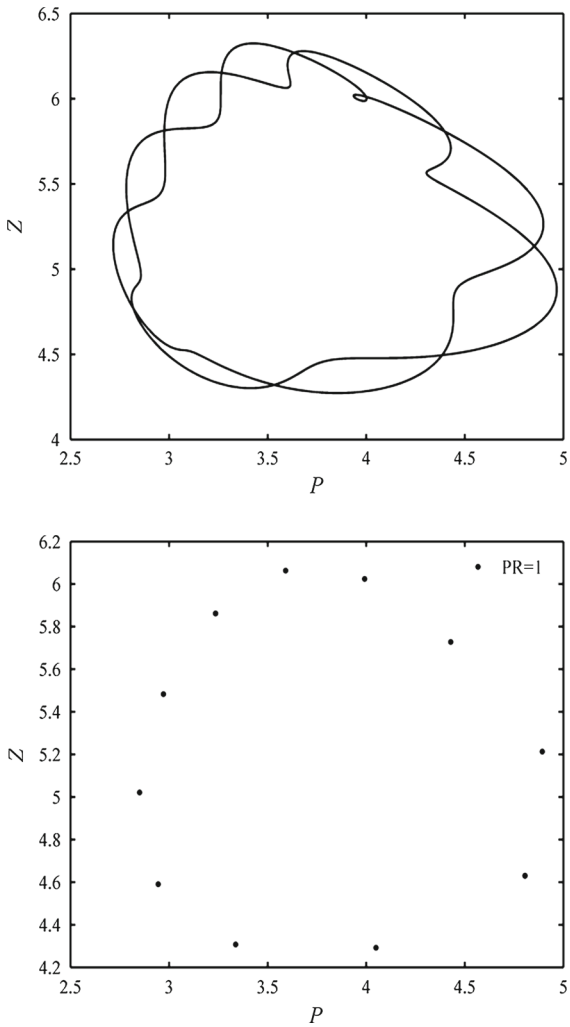

Fig. 1 Periodic oscillation of the ecological oscillatory system shown in phase diagram and Poincaré map. $u_0 = 0.01$, $w_1 = 0.02$, $w_2 = 0.11$. PR = 1

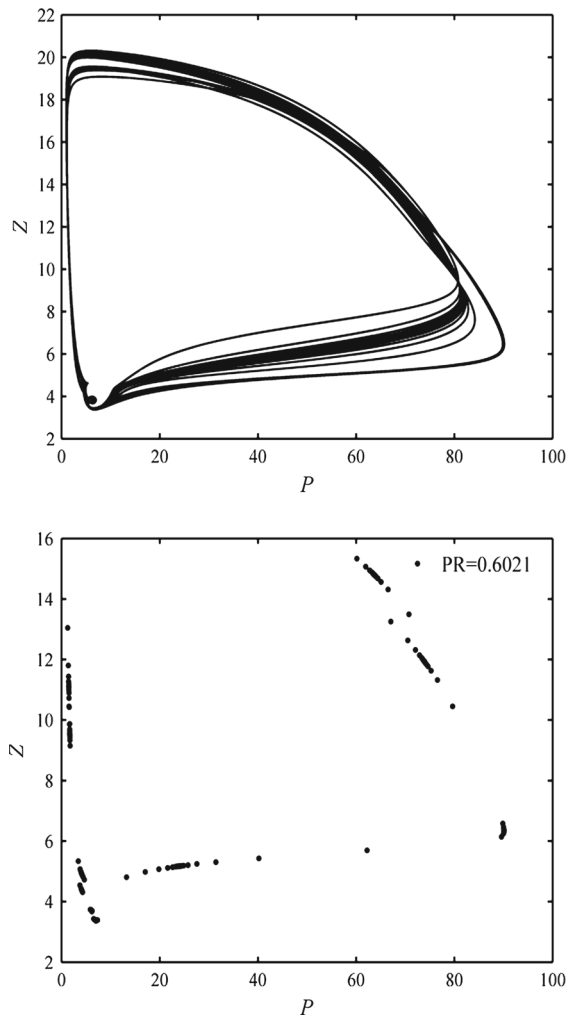

Fig. 2 Oscillation between periodic and quasiperiodic of the ecological oscillatory system shown in phase diagram and Poincaré map. $u_0 = 0.02$, $w_1 = 0.02$, $w_2 = 0.11$. PR = 0.6021

The characteristics of the different oscillations are described in phase diagrams and Poincaré maps, as can be visualized in Figs. 1, 2, 3, and 4. At the same time, the PR value is calculated for each case of dynamical oscillation.

Figure 1 shows a typical periodic oscillation of the system, as graphically described by the closed periodic orbits in the phase diagram and finite points in the Poincaré map. Using the method described in Sect. 2, the PR value for this oscillation is one. This implies a perfect periodic oscillation of the system, for this case.

Figure 2 shows the dynamical oscillation which is neither period nor quasiperiod or chaos. For such a case, dynamical characteristics of the system can be quantitatively described by the PR method. The PR value for this case is 0.6021, which reveals about sixty percent periodicity of the oscillation. As per the PR approach, the higher the PR value is, the more periodic is the dynamical oscillation [13].

The dynamical oscillation of Fig. 2 holds the properties of periodic and quasiperiodic oscillations simultaneously. As shown in the Poincaré map, the scattered overlapping points describe the periodicity, whereas the fractured curves suggest that the system also experiences quasiperiodicity. However, the system never settles down to a periodic or quasiperiodic attractor, but continues jumping between the two.

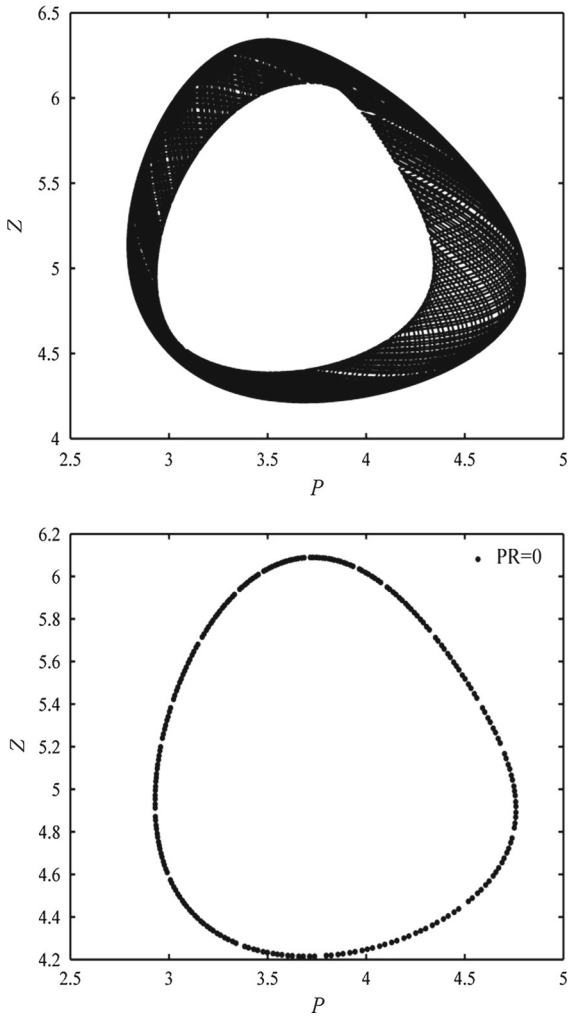

Fig. 3 Quasiperiodic oscillation of the ecological oscillatory system shown in phase diagram and Poincaré map. $u_0 = 0.01$, $w_1 = 2\pi/365$, $w_2 = 0.11$. PR = 0

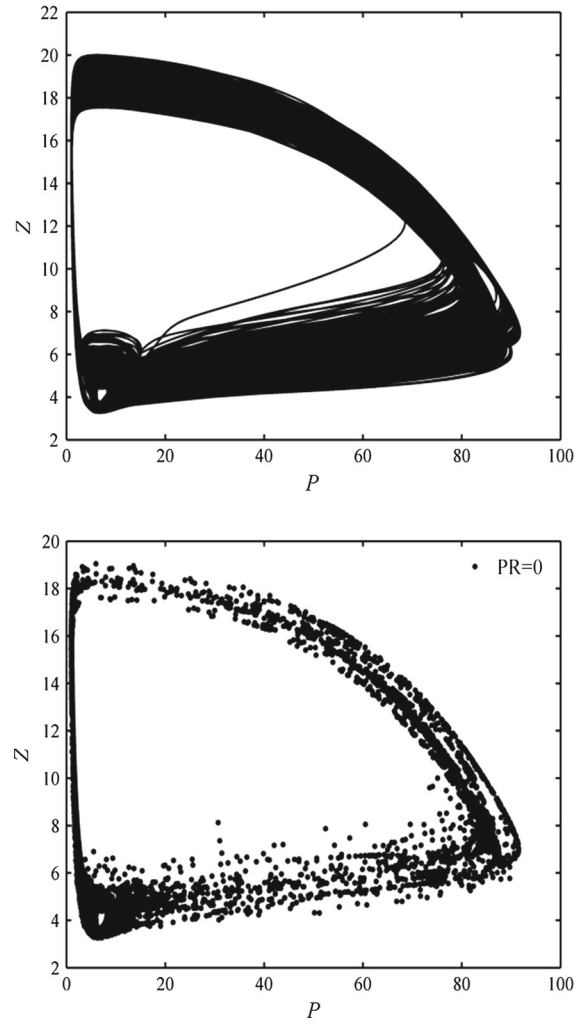

Fig. 4 Chaotic oscillation of the ecological oscillatory system shown in phase diagram and Poincaré map. $u_0 = 0.02$, $w_1 = 2\pi/365$, $w_2 = 0.21$. PR = 0

The existence of dynamical oscillations in between periodic and quasiperiodic can be supported by many research works in literature. For example, a type of dynamical behavior of nonlinear systems, almost periodic behavior, is found in literature [40,41]. Almost periodic behaviors are not perfect periodic and are neither quasiperiodic nor chaotic as well. Some researchers have proved that almost periodic behaviors are not transient states of nonlinear systems, but exist as attractors [42].

The quasiperiodic and chaotic oscillations of the system are also found for the system as described in Figs. 3 and 4. The quasiperiodic oscillation is graphically described by the Poincaré map of Fig. 3 which clearly shows a closed loop. And the Poincaré map of Fig. 4 shows a cloud with random like and irregularly distributed points, indicating a typical chaotic oscillation of the system. It should be noticed that the PR values for both cases are zero. The secondary Poincaré map therefore needs to be constructed for further distinguishing the two.

Using the PR values as a single index, the PR method can be applied to demonstrate the changes and distributions of different dynamical oscillations corresponding to a range of parameter values. As shown in the graphs of Fig. 5, the graphs of PR values corresponding to

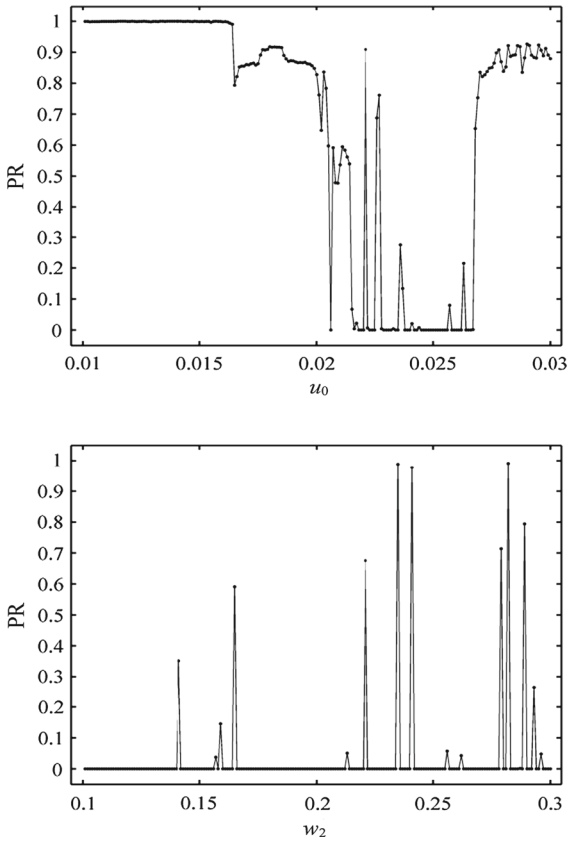

Fig. 5 Change of PR values with the parameters of u_0 ($w_1 = 0.02$, $w_2 = 0.21$) and w_2 ($u_0 = 0.01$, $w_1 = 2\pi/365$)

parameter variations (u_0 and w_2) are plotted. With the PR value graph, one may clearly see that the system responses periodically when $u_0 < 0.0165$ and then goes through transitional oscillations between periodic and quasiperiodic as u_0 increases. Further increasing u_0, the system mainly becomes quasiperiodic/chaotic and eventually returns to nearly periodic oscillations at larger u_0. Moreover, when $w_1 = 2\pi/365$, $u_0 = 0.01$, the system mainly shows quasiperiodic or chaotic oscillations as the parameter w_2 varies.

3.2 Application of secondary Poincaré map

In constructing the secondary Poincaré map, as indicated previously, the two groups of straight lines defined as Y and $\tilde{Y}$ in the Definitions 3 and 5 need to be selected. It should be noticed that in the map f_2, the selection of coefficients a and b is arbitrary. Therefore, for convenience of numerical simulations, the directions of the two groups of straight lines are selected as parallel to the axes, P and Z, of the Poincaré map, i.e., $b = 0$ for Y and $a = 0$ for $\tilde{Y}$.

According to the description in Sect. 2, the construction of the secondary Poincaré map can be divided into three steps, X_1, the visible points; X_2, the intermap of X_1 and Y; and X_3, the intermap of X_2 and $\tilde{Y}$. In numerical simulations, the graph X_1 is visually the same as that of the Poincaré map. Therefore, X_1 and the Poincaré map are merely shown in one graph.

Moreover, since the running time of the simulations cannot be infinite, the number of points in the Poincaré maps, k, can only be a finite number. However, the secondary Poincaré map is theoretically defined using the assumption that k approaches infinite. Therefore, for plotting the graphs X_2 and X_3 of the secondary Poincaré map, the map f_2 defined in Definition 5 is slightly modified as

$$f_2|_Y(X_1) = X_2 = \begin{cases} \bigcup_i (X_1 \cap Y_i) \text{ for all } i,\ N_i > n_0,\ 1 \le i \le s,\ i \in Z, & \text{if } N > n_0 \\ X_1 \cap Y_i \text{ for any } i,\ N_i = N,\ 1 \le i \le s,\ i \in Z, & \text{if } N \le n_0 \end{cases}, \tag{26}$$

in which N is modified as

$$N = \max_{1 \le i \le s} N_i, \tag{27}$$

and n_0 is a finite number. The same modification is also made for $X_3 = f_2|_{\tilde{Y}}(X_2)$ accordingly. The selection

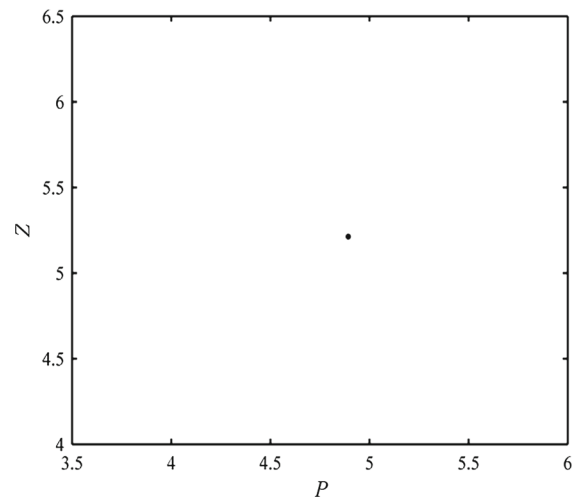

Fig. 6 Secondary Poincaré map (X_2 is equal to X_3) of the periodic oscillation. The parameter values are the same as that in Fig. 1. $C(X_0) = 4359$, $C(X_2) = 1$, $C(X_3) = 1$

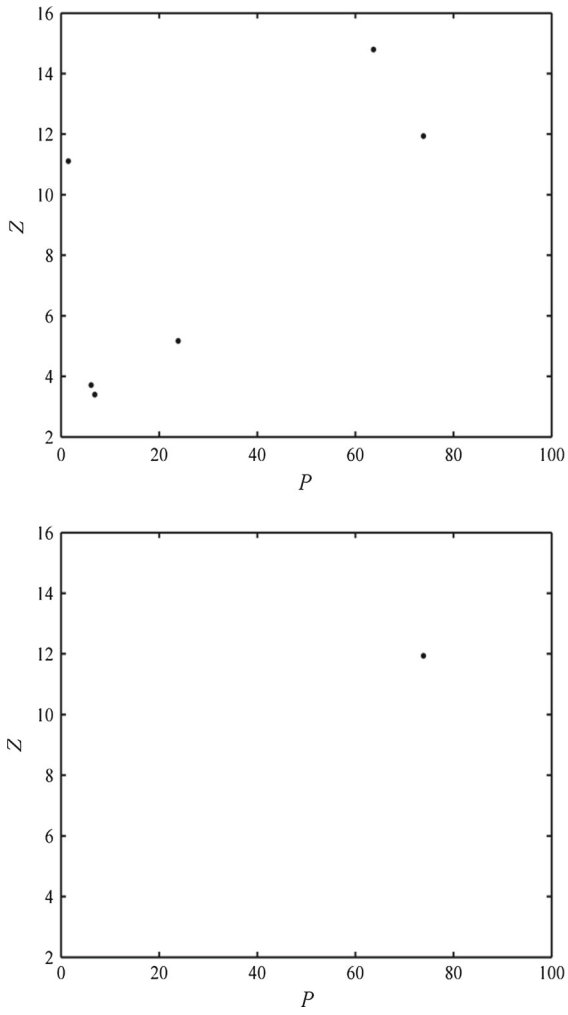

Fig. 7 Secondary Poincaré maps (X_2 and X_3) of the oscillation in between periodic and quasiperiodic. The parameter values are the same with Fig. 2. $C\,(X_0) = 4359$, $C\,(X_2) = 207$, $C\,(X_3) = 1$

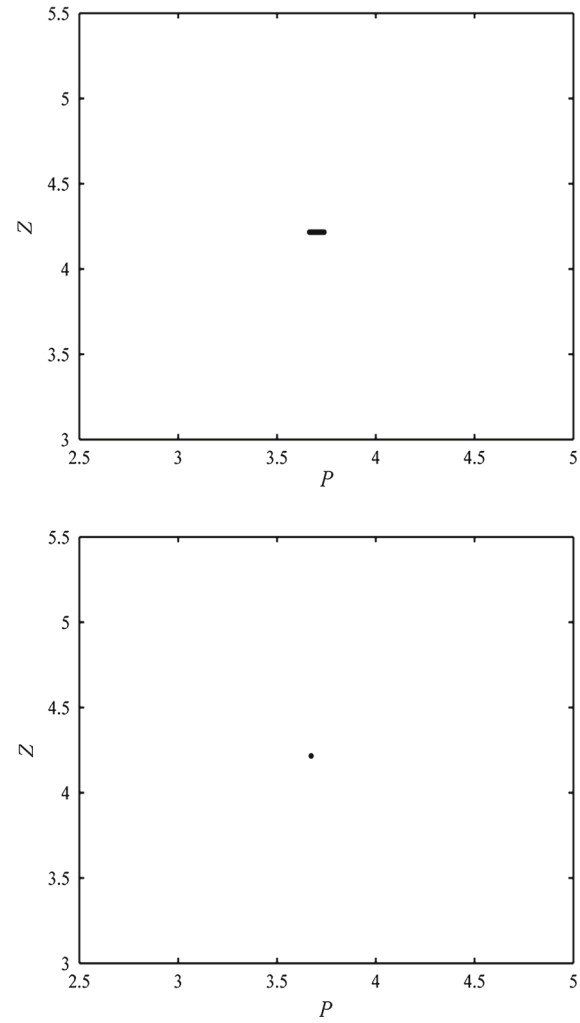

Fig. 8 Secondary Poincaré maps (X_2 and X_3) of the quasiperiodic oscillation shown in Fig. 3. $C\,(X_0) = 4359$, $C\,(X_2) = 14$, $C\,(X_3) = 1$

of the values for n_0 depends on the oscillatory system considered and the conditions applied in numerical simulations. In order to obtain proper and applicable value of n_0 for the ecological oscillatory system, all of the numerical simulations are performed under the same simulation conditions, including time step-size, running time, initial conditions, and time starting for sampling points for the Poincaré map. It should be noticed that the time interval selected for the secondary Poincaré maps depends on the value of parameter w_1 or w_2 and therefore is varying. After a number of testing simulations for various cases of the ecological oscillatory system considered, n_0 for $f_2|_Y$ is given as 12 and for $f_2|_{\tilde{Y}}$ is given as 5, and these values are used in the following numerical simulations.

Figure 6 shows that the periodic oscillation is rapidly reduced to a point in X_2. This is due to that the periodic oscillation shows several fixed points in X_1 (see the Poincaré map of Fig. 1). In Fig. 7, the oscillation in between periodic and quasiperiodic is reduced to several groups of points in X_2, and then the point groups become one point in X_3. Each group of points in X_2 is comprised of a few extremely close points and visualized just like as one point. Each point in X_2 represents an almost periodic point because the system repeatedly returns to the neighborhood of the point.

Figures 8 and 9 show the secondary Poincaré maps for the quasiperiodic oscillations. In Fig. 8, X_1 (see the Poincaré map of Fig. 3) just shows a circle, and the circle is reduced to a point after the steps of X_2 and X_3. In Fig. 9, the quasiperiodic oscillation forms a smooth loop in the Poincaré map (X_1), and this loop is reduced to a group of 5 points in X_3.

Figures 10 and 11 show the secondary Poincaré maps for chaotic oscillations of the system. It can be seen from the figures that scattered and isolated points are removed after the steps of X_2 and X_3. The left points in the graphs of X_3 form smaller dark areas. The dark areas are comprised of a great number of points, having about 26 % (Fig. 10) and 14 % (Fig. 11) of $C\ (X_0)$.

In comparison with Figs. 6, 7, 8, 9, 10 and 11, the number of points in X_3 of chaotic oscillations is much larger than that of any other cases, totally not on the same order of magnitude. Nevertheless, from the viewpoint of practical simulations which can only be finite in time and domain, a diagnosing criterion that can be used to distinguish chaos from quasiperiodic and periodic cases should be established. Specifically in numer-

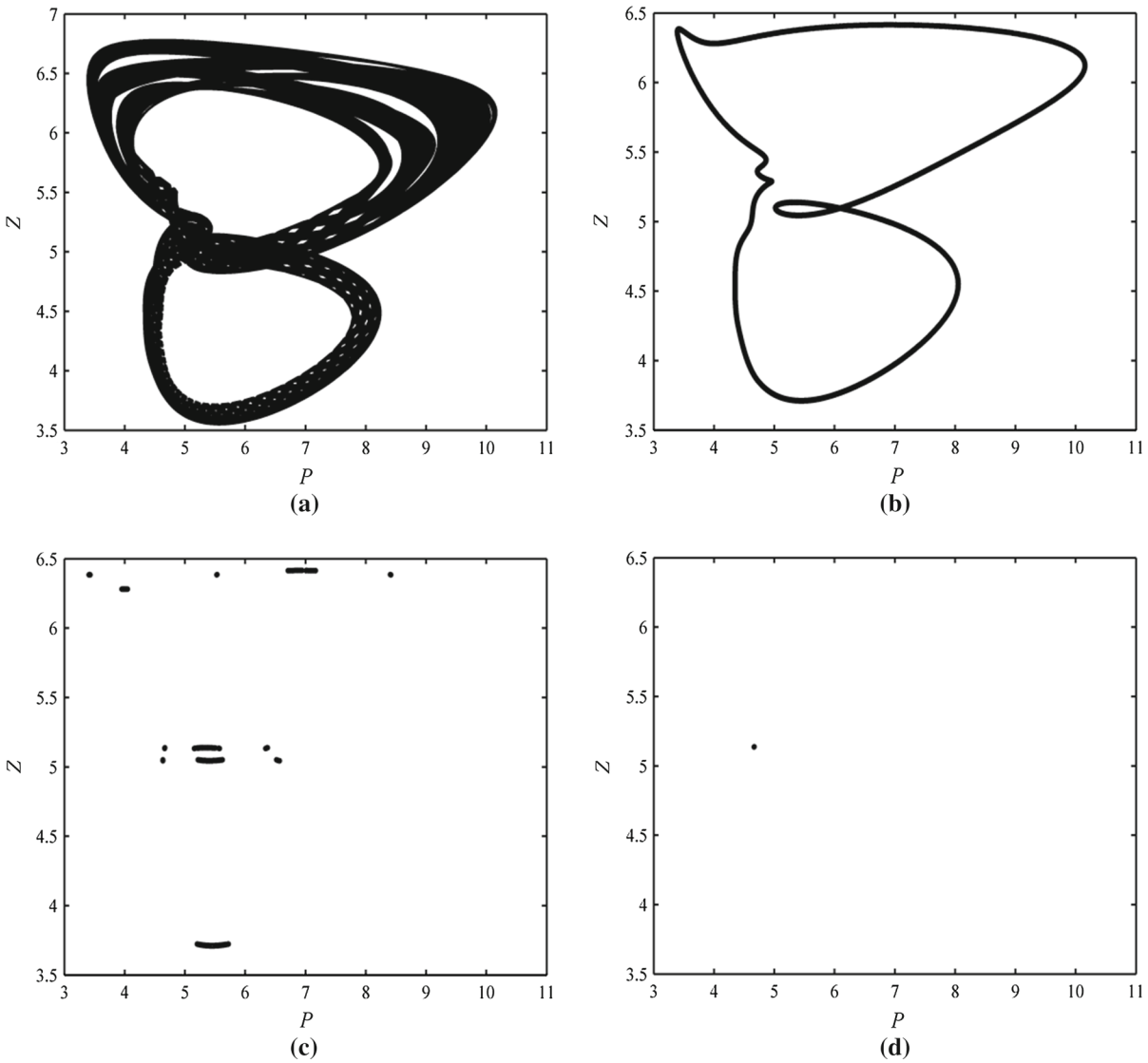

Fig. 9 A quasiperiodic oscillation shown in **a** phase diagram, **b** Poincaré map, and secondary Poincaré maps, **c** X_2 and **d** X_3. $u_0 = 0.017$, $w_1 = 2\pi/365$, $w_2 = 0.17$. $C\ (X_0) = 6737$, $C\ (X_2) = 556$, $C\ (X_3) = 5$

ical simulation practices, $C\,(X_3)$ in the case of chaos should be distinguishably large in comparison with that of quasiperiodic and periodic cases.

In fact, based on the nature of $C(X_3)$ defined and the time duration by which periodic and quasiperiodic responses of the system can be diagnosed, $C\,(X_3)$ of chaotic cases is substantially larger than that of quasiperiodic and periodic cases. For the system studied in this research, as shown in Fig. 12, when $\log_{10}(C\,(X_3))$ is less than one, the system follows periodic and quasiperiodic oscillations and the oscillations in between the periodic and quasiperiodic. When the system follows non-chaotic oscillations, the value of $C\,(X_3)$ stays at 2 in over ninety percent cases. Therefore, this value is taken as the base value of $C\,(X_3)$ for non-chaotic oscillations. When $\log_{10}(C\,(X_3))$ is near or larger than 3, it can be seen in Fig. 12, and the value of $C\,(X_3)$ is at least 450 times larger than the base value of non-chaotic oscillations. With such a large $C\,(X_3)$, the corresponding responses of the system are chaos as can be proved by phase diagram or regular Poincaré map. With this comparison, a large enough threshold say a number greater than 200 can be easily identified and used for numerical diagnosing practice to distinguish chaos from non-chaotic cases.

3.3 Periodic–quasiperiodic–chaotic region diagrams

The PR method may quantitatively diagnose the periodic and quasiperiodic oscillations and oscillations in between the two, as shown in Fig. 5, whereas the secondary Poincaré map may be used to distinguish the quasiperiodic and chaotic oscillations, as shown in Fig. 12. Combining the two methods, the entire dynamical characteristics of nonlinear oscillatory systems can be systemically and completely diagnosed within a desired range of system parameter values.

The periodic–quasiperiodic–chaotic region diagrams have shown great significances in analyzing the nonlinear behaviors of dynamic systems [13]. With the approach combining the two methods of PR method and secondary Poincaré map approach, the periodic–quasiperiodic–chaotic region diagrams can be conveniently generated with consideration of large system parameter ranges. For the system considered in the present research, two periodic–quasiperiodic–chaotic region diagrams are plotted as shown in Fig. 13. In the region diagrams, the regions of periodic (diamonds

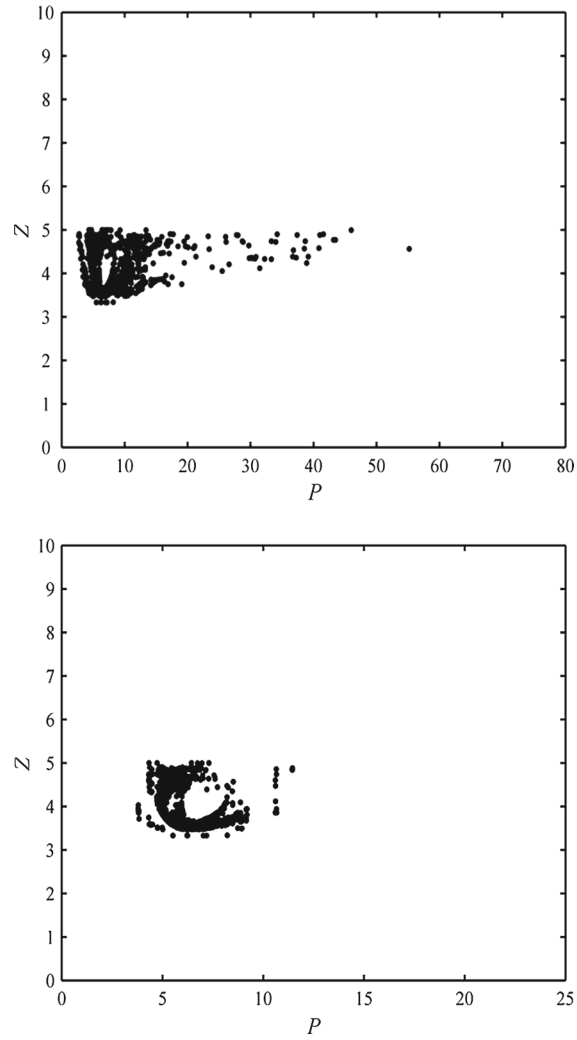

Fig. 10 Secondary Poincaré maps X_2 and X_3 of the chaotic oscillation shown in Fig. 4. $C\,(X_0) = 8322, C\,(X_2) = 2787, C\,(X_3) = 2175$

in the diagram), quasiperiodic (sign of "+"), chaotic (stars) oscillations and the oscillations in between the periodic and quasiperiodic (white blank areas) of the ecological oscillatory system can be easily identified. It should be noticed that each point in the diagrams actually represents a state of the system corresponding to the given parameter values.

The periodic–quasiperiodic–chaotic diagrams present global distributions of the dynamical behaviors for the system studied and provide a powerful tool for identifying and analyzing the behaviors of the nonlinear system. As shown in Fig. 13, the chaotic oscillations are distributed in the area where parameter u_0

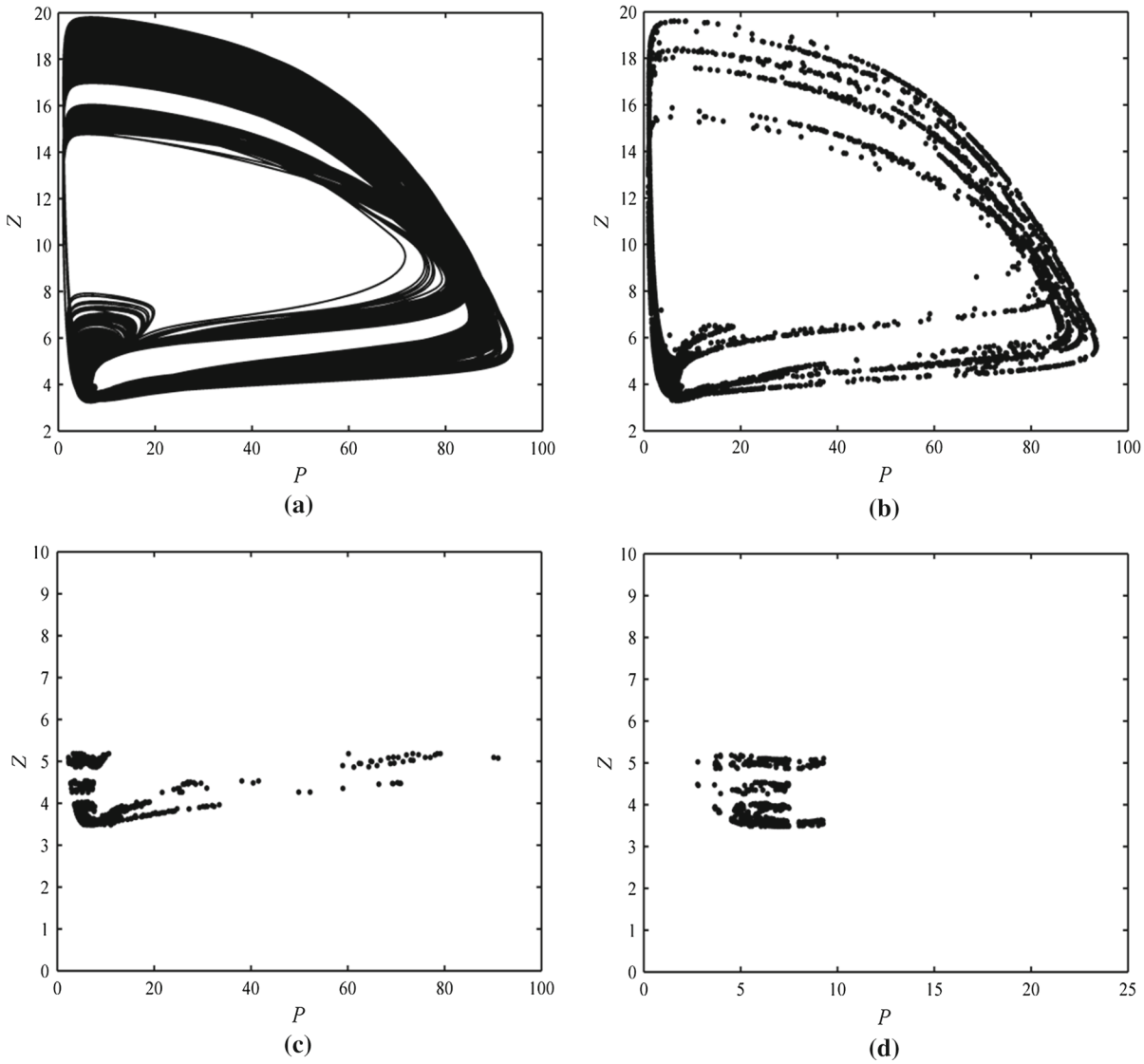

Fig. 11 A chaotic oscillation shown in **a** phase diagram, **b** Poincaré map, and secondary Poincaré maps, **c** X_2 and **d** X_3. $u_0 = 0.025$, $w_1 = 2\pi/365$, $w_2 = 0.25$. $C(X_0) = 7925$, $C(X_2) = 1578$, $C(X_3) = 1118$

has relatively high values, in the range 0.019–0.022 for Fig. 13a and 0.0214–0.022 for Fig. 13b. Moreover, the region diagrams allow simultaneous comparison of different types of oscillations of the system corresponding to large ranges of system parameters. As can be seen from Fig. 13a when the value of w_1 is $2\pi/365$, the appearance of quasiperiodic and chaotic oscillations dominates, whereas no periodic oscillation takes place. In Fig. 13b when the value of w_1 is 0.02, the system almost completely follows the periodic oscillation and the oscillations in between periodic and quasiperiodic, whereas the quasiperiodic and chaotic oscillations scarcely emerge.

4 Discussion and conclusion

This research establishes an approach for diagnosing the complex characteristics of nonlinear dynamical systems with a secondary Poincaré map approach combined with the PR method. Previously some research works have been done, where the quasiperiodic oscil-

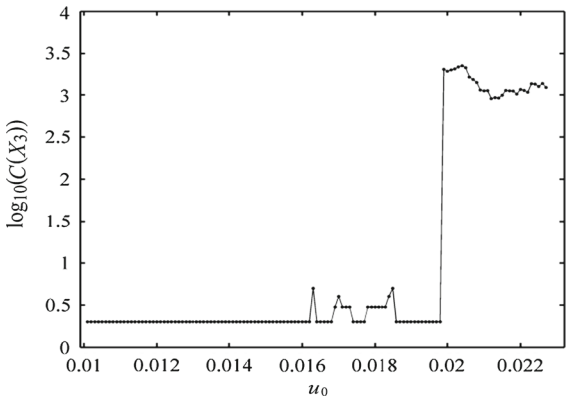

Fig. 12 Change of logarithm of number of points in X_3 with parameter u_0. $w_1 = 2\pi/365$, $w_2 = 0.2$

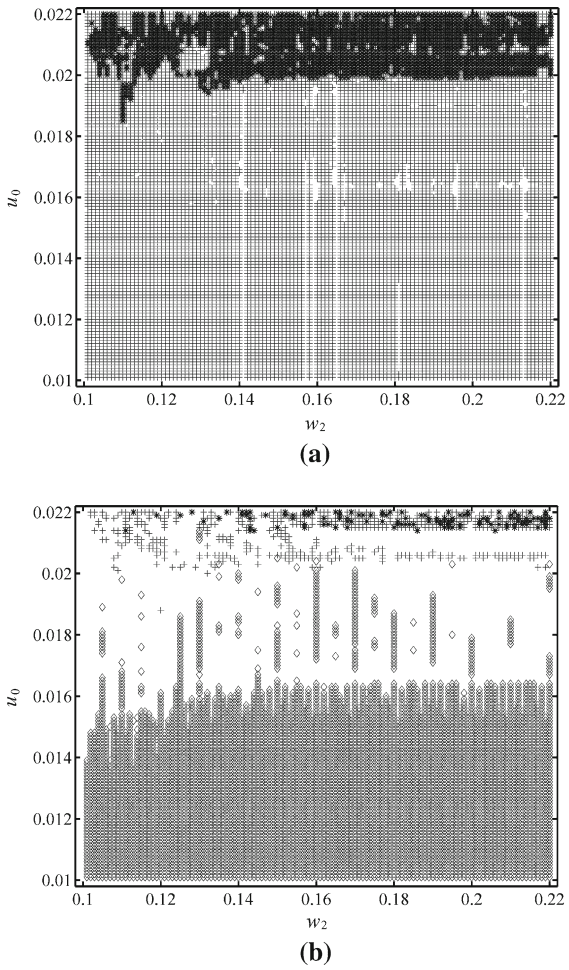

Fig. 13 Periodic–quasiperiodic–chaotic region diagrams corresponding to varying parameters w_2 and u_0. **a** $w_1 = 2\pi/365$, **b** $w_1 = 0.02$

lation was reduced to a fixed point. In comparison with the existing approaches, which reduce quasiperiodic oscillation to a fixed point in a map, the present approach maps all types of dynamical responses with considerations of the structures of the responses in the corresponding Poincaré map. This provides the availability of a complete diagnosis with higher accuracy and efficiency for the nonlinear behaviors of dynamical systems.

The present approach shows improvement in the former Ueda's and Khammari's approach. The works of Ueda and Khammari et al. play an important role in nonlinear characteristics diagnosis [32,33]. Their Poincaré mapping method provides effectiveness and is widely cited for diagnosing the nonlinear behaviors of dynamical systems such as chaos and periodicity. However, it should be noticed that Ueda's diagram of diagnosis results is created with the observation of Poincaré maps and phase diagrams for each of the cases considered. This may lead to incomplete diagnosis, for example, quasiperiodic cases are not considered in the Ueda's diagram. In contrast to the approach of Ueda and Khammari et al., the combined approach in this research is based on single value index, which can quantitatively diagnose the nonlinear behaviors of dynamical systems, without plotting and observing a great deal of figures of Poincare maps or phases diagrams.

The following aspects are discussed and addressed for the application of the present approach to diagnose the nonlinear behaviors of dynamical systems.

1. For periodically forced systems, the method of constructing Poincaré sections as described in Sect. 2 can be applied, whereas for the nonlinear oscillatory systems without periodic force, many other methods in literature can also be applied to construct the Poincaré sections, such as the research works of Thompson and Stewart, Letellier and Gilmore, and Dai and Wang [43–45]. Based on the Poincaré sections constructed, the PR values for oscillatory systems can still be determined, as shown in Dai and Wang [45].
2. The proposed combined approach is applied for diagnosing the nonlinear behaviors of the periodically forced systems, such as Duffing system, seasonally perturbed predator–prey systems [7,8,32,33,46]. For the periodically forced dynam-

ical systems described by Eq. (1), the effective dimension is three and the third dimension is introduced by the periodically forced term [33]. Therefore, two-dimensional periodically forced dynamical systems can also exhibit chaotic behaviors. For example, the chaotic oscillations in Duffing system have been widely studied [2,3,24,32]. Gao et al. studied a two-dimensional periodically forced phytoplankton–zooplankton system and found chaos [38]. The application in Sect. 3 also focuses on the Gao's system. Using the same parametric conditions, the combined approach can determine same quasiperiodic and chaotic behaviors that Gao et al. claimed. This proves effectiveness and feasibility of applying the combined approach to the periodically forced systems.

3. The approach presented in the research is based on numerical computation, and thus the results are related to computational accuracy. Therefore, applying the approach to diagnose nonlinear characteristics of dynamical systems demands validation to give proper values for numerical parameters, such as running time, error tolerance, and so on. These numerical parameter values determine the computational accuracy for PR values and secondary Poincaré map. Based on the validation, a reliable application of the combined approach to new nonlinear systems can be achieved.

With the findings of the research, the following can be concluded.

1. With the secondary Poincaré map approach, theoretically, the periodic and quasiperiodic oscillations and the oscillations in between periodic and quasiperiodic can be reduced to finite points in a new map, whereas chaotic oscillations have infinite points in the map though the structure of the points is stable. Numerically, in chaotic cases, the number of points in the secondary Poincaré map has a much higher order of magnitude in comparison with that of the other cases. Thus, chaos can be conveniently distinguished from quasiperiodic and periodic responses or the responses in between.
2. The PR method is effective in quantifying the periodicity of a nonlinear response. Significantly, the PR method defines the characteristics in between the periodic and quasiperiodic oscillations, which is difficult to determine with employment of any other methods. However, the PR method cannot be used to directly distinguish chaos and quasiperiodicity of a system. As shown in the research, the PR method and secondary Poincaré map approach are inter-complementary. Combination of the two methods provides the advantage of systematically and completely diagnosing the entire dynamical behaviors of nonlinear oscillatory systems.
3. The periodic–quasiperiodic–chaotic region diagrams can be numerically generated without plotting any diagrams such as wave or phase diagram or Poincaré map, corresponding to the system parameters of desired ranges.
4. An ecological oscillatory system is studied with employment of the combined approach of the secondary Poincaré map and PR methods. The approach shows high applicability and efficiency in numerically diagnosing the nonlinear behaviors of dynamic systems. The periodic–quasiperiodic–chaotic region diagrams generated with utilization of the approach developed provide global picture of the behaviors of the ecological system. It should be noticed that, with the approach developed in this research, the region diagrams of the other system parameters can also be created as desired.

Acknowledgments The authors would like to acknowledge with great gratitude for the supports of Chinese Natural Science Foundation (Project 39560023 to H.Z.), National Special Water Programs (No. 2009ZX07210-009, No. 2015ZX07203-011, No. 2015ZX07204-007), Department of Environmental Protection of Shandong Province (SDHBPJ-ZB-08), the China Scholarship Council (No. 201206730024), and the University of Regina.

References

1. Lee, W.K., Park, H.D.: Chaotic dynamics of a harmonically excited spring-pendulum system with internal resonance. Nonlinear Dyn. **14**, 211–229 (1997)
2. Fang, T., Dowell, E.H.: Numerical simulations of periodic and chaotic responses in a stable duffing system. Int. J. Non-Linear Mech. **22**, 401–425 (1987)
3. Jing, Z., Wang, R.: Complex dynamics in Duffing system with two external forcings. Chaos Solitons Fractals **23**, 399–411 (2005)
4. Trejo-Guerra, R., Tlelo-Cuautle, E., Jiménez-Fuentes, J.M., Sánchez-López, C., Muñoz-Pacheco, J.M., Espinosa-Flores-Verdad, G., Rocha-Pérez, J.M.: Integrated circuit generating 3- and 5-scroll attractors. Commun. Nonlinear Sci. Numer. Simul. **17**, 4328–4335 (2012)
5. Tlelo-Cuautle, E., Rangel-Magdaleno, J.J., Pano-Azucena, A.D., Obeso-Rodelo, P.J., Nuñez-Perez, J.C.: FPGA realization of multi-scroll chaotic oscillators. Commun. Nonlinear Sci. Numer. Simul. **27**, 66–80 (2015)

6. Rinaldi, S., Muratori, S.: Conditioned chaos in seasonally perturbed predator-prey models. Ecol. Model. **69**, 79–97 (1993)
7. Gakkhar, S., Naji, R.K.: Chaos in seasonally perturbed ratio-dependent prey-predator system. Chaos Solitons Fractals **15**, 107–118 (2003)
8. Rinaldi, S., Muratori, S., Kuznetsov, Y.: Multiple attractors, catastrophes and chaos in seasonally perturbed predator-prey communities. Bull. Math. Biol. **55**, 15–35 (1993)
9. Strogatz, S.H.: Nonlinear Dynamics and Chaos-With Applications to Physics, Biology, Chemistry and Engineering, 1st edn. Addison-Wesley, Boston (1994)
10. Dai, L., Wang, G.: Implementation of periodicity-ratio in analyzing nonlinear dynamic systems: a comparison with Lyapunov-exponent. J. Comput. Nonlinear Dyn. **3**, 011006.1–011006.9 (2008)
11. Hastings, A., Powell, T.: Chaos in a three-species food chain. Ecology **72**, 896–903 (1991)
12. Nayfeh, A.H., Balachandran, B.: Applied Nonlinear Dynamics: Analytical, Computational, and Experimental Methods. Wiley Interscience, New York (1995)
13. Dai, L.: Nonlinear Dynamics of Piecewise Constant Systems and Implementation of Piecewise Constant Arguments. World Scientific Publishing Co., New Jersey (2008)
14. Parker, T.S., Chua, L.O.: Chaos: a tutorial for engineers. Proc. IEEE **75**, 982–1008 (1987)
15. Wolf, A., Swift, J.B., Swinney, H.L., Vastano, J.A.: Determining Lyapunov exponents from a time series. Phys. D Nonlinear Phenom. **16**, 285–317 (1985)
16. Pecora, L.M., Carroll, T.L.: Synchronization in chaotic systems. Phys. Rev. Lett. **64**, 821–824 (1990)
17. Yang, C.J., Zhu, W.D., Ren, G.X.: Approximate and efficient calculation of dominant Lyapunov exponents of high-dimensional nonlinear dynamic systems. Commun. Nonlinear Sci. Numer. Simul. **18**, 3271–3277 (2013)
18. Carbajal-Gómez, V.H., Tlelo-Cuautle, E., Fernández, F.V.: Optimizing the positive Lyapunov exponent in multi-scroll chaotic oscillators with differential evolution algorithm. Appl. Math. Comput. **219**, 8163–8168 (2013)
19. Chlouverakis, K.E., Sprott, J.C.: A comparison of correlation and Lyapunov dimensions. Phys. D Nonlinear Phenom. **200**, 156–164 (2005)
20. Leonov, G.A.: Lyapunov functions in the attractors dimension theory. J. Appl. Math. Mech. **76**, 129–141 (2012)
21. Bonakdar, M., Samadi, M., Salarieh, H., Alasty, A.: Stabilizing periodic orbits of chaotic systems using fuzzy control of Poincaré map. Chaos Solitons Fractals **36**, 682–693 (2008)
22. Mukherjee, S., Palit, S.K., Bhattacharya, D.K.: Is one dimensional Poincaré map sufficient to describe the chaotic dynamics of a three dimensional system? Appl. Math. Comput. **219**, 11056–11064 (2013)
23. Tucker, W.: Computing accurate Poincaré maps. Phys. D **171**, 127–137 (2002)
24. Dai, L., Singh, M.C.: Diagnosis of periodic and chaotic responses in vibratory systems. J. Acoust. Soc. Am. **102**, 3361–3371 (1997)
25. Ott, E.: Chaos in Dynamical Systems. Cambridge University Press, Cambridge (2002)
26. Olga, I., Moskalenkoa, O., Koronovskii, A., Hramova, A., Zhuravleva, M., Levina, Y.: Cooperation of deterministic and stochastic mechanisms resulting in the intermittent behavior. Chaos Solitons Fractals **68**, 58–64 (2014)
27. Miller, R.K.: Almost periodic behavior of solutions of a nonlinear Volterra system. Brown UNIV Providence RI DIV of Applied Mathematics (1969)
28. Xia, Y., Cao, J.: Almost periodicity in an ecological model with M-predators and N-preys by pure-delay type system. Nonlinear Dyn. **39**, 275–304 (2005)
29. Abbas, S., Sen, M., Banerjee, M.: Almost periodic solution of a non-autonomous model of phytoplankton allelopathy. Nonlinear Dyn. **67**, 203–214 (2012)
30. Kaas-Petersen, C.: Computation of quasi-periodic solutions of forced dissipative systems. J. Comput. Phys. **58**, 395–408 (1985)
31. Kaas-Petersen, C.: Computation, continuation, and bifurcation of torus solutions for dissipative maps and ordinary differential equations. Phys. D Nonlinear Phenom. **25**, 288–306 (1987)
32. Ueda, Y.: Steady motions exhibited by Duffing's equation: a picture book of regular and chaotic motions. Presented at the Engineering Foundation Conference on New Approaches to Nonlinear Problems in Dynamics, Monterey, CA, 9–14 Dec. 1979, vol 1, 9–14 (1980)
33. Khammari, H., Mira, C., Carcassés, J.P.: Behavior of harmonics generated by a duffing type equation with a nonlinear damping: part I. Int. J. Bifurc. Chaos **15**(10), 3181–3221 (2005)
34. Dai, L., Han, L.: Analysing periodicity, nonlinearity and transitional characteristics of nonlinear dynamic systems with Periodicity Ratio (PR). Commun. Nonlinear Sci. Numer. Simul. **16**, 4731–4744 (2011)
35. Moon, F.C.: Chaotic and Fractal Dynamics: Introduction for Applied Scientists and Engineers. Wiley, New York (2008)
36. Scheffer, M., Rinaldi, S., Kuznetsov, Y.A., van Nes, E.H.: Seasonal dynamics of Daphnia and algae explained as a periodically forced predator-prey system. Oikos **80**, 519–532 (1997)
37. Edwards, A.M., Brindley, J.: Oscillatory behavior in a three-component plankton population model. Dyn. Stab. Syst. **11**, 389–413 (1996)
38. Gao, M., Shi, H., Li, Z.: Chaos in a seasonally and periodically forced phytoplankton–zooplankton system. Nonlinear Anal. Real World Appl. **10**, 1643–1650 (2009)
39. Truscott, J.E., Brindley, J.: Ocean plankton populations as excitable media. Bull. Math. Biol. **56**, 981–998 (1994)
40. Duan, L., Huang, L., Guo, Z.: Stability and almost periodicity for delayed high-order Hopfield neural networks with discontinuous activations. Nonlinear Dyn. **77**, 1469–1484 (2014)
41. Xia, Y., Cao, J., Zhang, H., Chen, F.: Almost periodic solutions of n-species competitive system with feedback controls. J. Math. Anal. Appl. **294**, 503–522 (2004)
42. Xia, Y., Han, M., Huang, Z.: Global attractivity of an almost periodic N-species nonlinear ecological competitive model. J. Math. Anal. Appl. **337**, 144–168 (2008)
43. Thompson, J.M.T., Stewart, H.B.: Nonlinear Dynamics and Chaos. Wiley, New York (2002)
44. Letellier, C., Gilmore, R.: Poincaré sections for a new three-dimensional toroidal attractor. J. Phys. A Math. Theor. **42**, 015101 (2009)

45. Dai, L., Wang, X.: Diagnosis of nonlinear oscillatory behavior of a fluttering plate with a periodicity ratio approach. Nonlinear Eng. **1**, 67–75 (2012)

46. Upadhyay, R.K., Iyengar, S.R.K.: Effect of seasonality on the dynamics of 2 and 3 species prey-predator systems. Nonlinear Anal. Real World Appl. **6**, 509–530 (2005)